© 2017. Published by The Company of Biologists Ltd | Development (2017) 144, 321-333 doi:10.1242/dev.147462

RESEARCH ARTICLE

An Epha4/Sipa1l3/Wnt pathway regulates eye development and lens maturation

Melanie Rothe[1,2,*], Noreen Kanwal[2,3,*], Petra Dietmann[1], Franziska A. Seigfried[1,2], Annemarie Hempel[1,2], Desiree Schütz[1], Dominik Reim[2,3], Rebecca Engels[1], Alexander Linnemann[1], Michael J. Schmeisser[3,4], Juergen Bockmann[3], Michael Kühl[1], Tobias M. Boeckers[3,‡] and Susanne J. Kühl[1,‡]

ABSTRACT

The signal-induced proliferation-associated family of proteins comprises four members, SIPA1 and SIPA1L1-3. Mutations of the human *SIPA1L3* gene result in congenital cataracts. In *Xenopus*, loss of Sipa1l3 function led to a severe eye phenotype that was distinguished by smaller eyes and lenses including lens fiber cell maturation defects. We found a direct interaction between Sipa1l3 and Epha4, building a functional platform for proper ocular development. Epha4 deficiency phenocopied loss of Sipa1l3 and rescue experiments demonstrated that Epha4 acts upstream of Sipa1l3 during eye development, with both Sipa1l3 and Epha4 required for early eye specification. The ocular phenotype, upon loss of either Epha4 or Sipa1l3, was partially mediated by *rax*. We demonstrate that canonical Wnt signaling is inhibited downstream of Epha4 and Sipa1l3 during normal eye development. Depletion of either Sipa1l3 or Epha4 resulted in an upregulation of *axin2* expression, a direct Wnt/β-catenin target gene. In line with this, Sipa1l3 or Epha4 depletion could be rescued by blocking Wnt/β-catenin or activating non-canonical Wnt signaling. We therefore conclude that this pathomechanism prevents proper eye development and maturation of lens fiber cells, resulting in congenital cataracts.

KEY WORDS: Epha4, Sipa1l3, Spar3, Wnt, Eye development, *Xenopus*

INTRODUCTION

The most common cause of blindness worldwide is a congenital or acquired cataract characterized by non-transparent opaque lenses (Churchill and Graw, 2011). On a molecular and cellular level, a congenital cataract can be caused by the loss of expression of lens-specific proteins such as crystallins, the presence of light-scattering organelles (i.e. nucleus, ER, mitochondria), disturbed cell adhesion or disorganized cytoskeleton. There are specific gene mutations known to cause congenital cataracts (Gupta et al., 2014), such as mutations in the Ephrin receptor tyrosine kinase, EPH receptor A2 (*EPHA2*), and its ligand Ephrin A5 (*EFNA5*). Both play a crucial role in lens development and *Epha2* or *Efna5* knockout mice develop cataracts (Shi et al., 2012; Jun et al., 2009; Cooper et al., 2008).

The mature lens consists of five major regions: (1) the lens epithelium that is located at the anterior pole of the lens, (2) the germinative zone where epithelial cells proliferate, (3) the lens equator where epithelial cells migrate, (4) the transition zone where lens fiber cells (LFCs) undergo cell cycle arrest and differentiation and (5) the lens center where the mature LFCs form the bulk of the lens. The lens epithelium serves as a stem cell niche for LFCs. Main features of mature LFCs are their elongated shape, the expression of transparent proteins, the crystallins, and the lack of organelles. An elastic lens capsule containing collagen surrounds the lens (Lovicu and McAvoy, 2005; Lovicu et al., 2011; Martinez and de Iongh, 2010; Wederell and de Iongh, 2006; Wride, 2011).

Development of the lens is tightly linked to normal eye development. The vertebrate eye arises as an optic vesicle from the neural tube and evaginates towards the overlaying ectoderm, in which it induces the lens placode. As development proceeds, the distal part of the eye vesicle invaginates and forms the bi-layered optic cup including the thinner outer retinal pigmented epithelium (RPE) and the thicker neural retina. Simultaneously, the lens placode invaginates, forming the lens vesicle. At the posterior side of the lens vesicle, cells begin to elongate towards the anterior side and start to express transparent proteins such as CRYAA, CRYAB and CRYG.

Recently, the *SIPA1L3* gene has also been associated with congenital human cataracts (Evers et al., 2015; Greenlees et al., 2015). SIPA1L3 is a member of the signal-induced proliferation-associated [SIPA, also known as the spine-associated rap-gap (SPAR)] proteins. In rodents, this protein family comprises four members, Sipa (or Spa1), Sipa1l1 (or Spar1), Sipa1l2 (or Spar2) and Sipa1l3 (or Spar3) (Spilker and Kreutz, 2010). All Sipa family members share common domains, namely an N-terminal RapGAP domain (Rap-GTPase activating domain), a PDZ domain and a C-terminal coiled-coil domain that was found to harbor a leucine zipper (Wendholt et al., 2006). So far, Sipa1l1-3 have been analyzed mainly with respect to their synaptic function in the central nervous system (Dolnik et al., 2016; Pak et al., 2001; Spilker et al., 2008).

Interestingly, Sipa1l1 was found to interact with the Ephrin receptor family member Epha4 via its PDZ domain. This interaction promotes phosphorylation of Sipa1l1 and an inactivation of the small GTPases Rap1 and Rap2 (Richter et al., 2007). Ephrin receptor tyrosine kinases are generally involved in cell recognition, adhesion, axonal pathfinding, growth cone mobility and/or morphology and cataract formation (Huot, 2004; Pasquale, 2005).

Besides its expression in the rodent brain, Sipa1l3 is also localized in the developing eye in humans, mice, frog and zebrafish, especially within the lens (Evers et al., 2015; Greenlees et al., 2015; Lachke et al., 2012; Rothe et al., 2016). In 2015, two groups independently showed that mutations of the human *SIPA1L3* gene are related to congenital cataracts. Some of the patients with homozygous or heterozygous mutations within *SIPA1L3* also showed microphthalmia (smaller

[1]Institute of Biochemistry and Molecular Biology, Ulm University, Ulm 89081, Germany. [2]International Graduate School in Molecular Medicine Ulm, Ulm University, Ulm 89081, Germany. [3]Institute for Anatomy and Cell Biology, Ulm University, Ulm 89081, Germany. [4]Department of Neurology, Ulm University, Ulm 89081, Germany.
*These authors contributed equally to this work

‡Authors for correspondence (tobias.boeckers@uni-ulm.de; susanne.kuehl@uni-ulm.de)

Received 24 November 2016; Accepted 6 December 2016

Development (2017) 144, 321-333 doi:10.1242/dev.147462

eyes) and anterior segment dysgenesis (Evers et al., 2015; Greenlees et al., 2015). In cell culture as well as in a mouse model, loss of Sipa1l3 interferes with cell polarity and cytoskeletal organization. This implies that loss of Sipa1l3 might contribute to cataract formation (Greenlees et al., 2015). However, the signaling cascades affected after Sipa1l3 depletion have not been identified so far.

In the search for a pathomechanism, we focused on molecular pathways involving Sipa1l3 during ocular development. As congenital cataracts and the microphthalmia phenotype must be caused by alterations that occur during early embryogenesis, we chose to carry out our studies in *Xenopus laevis*, a model that allows for easy examination of early embryogenesis. We showed that downregulation of Sipa1l3 in the *Xenopus* developing eye closely phenocopied the developmental defects of the eye, and especially the lens defects, that have been observed by others in mouse and zebrafish (Greenlees et al., 2015). Intriguingly, we identified a molecular and functional interaction between Sipa1l3 and Epha4 *in vivo*. Accordingly, Epha4 depletion resulted in an ocular phenotype that was similar to the loss of Sipa1l3. Furthermore, synergy and rescue experiments showed that Sipa1l3 acts downstream of Epha4. Additionally, both Sipa1l3 and Epha4 are required for eye specification and the eye phenotype upon Epha4 or Sipa1l3 deficiency is partially mediated by the important early eye development transcription factor *rax*. In addition, the Sipa1l3/Epha4 interaction is required to balance canonical and non-canonical Wnt signaling to regulate ocular development.

RESULTS

Sipa1l3 depletion causes ocular defects in *Xenopus laevis*

To analyze the molecular function of Sipa1l3 during vertebrate ocular development, we investigated Sipa1l3 in *Xenopus*. First, we determined the spatiotemporal expression pattern of *sipa1l3* using an antisense RNA probe. As we have shown previously (Rothe et al., 2016) and as observed in mouse and zebrafish (Greenlees et al., 2015; Lachke et al., 2012), *sipa1l3* transcripts were clearly detectable in the developing *Xenopus* eye including the early anterior neural plate where the eye field is localized (Fig. 1A, upper row, white arrowheads). In transverse sections of stained late tailbud embryos, *sipa1l3* is strongly expressed in the retina (Fig. 1B, upper row, black arrowhead) and lens epithelium (Fig. 1B, upper row, red arrowhead).

We further examined the role of Sipa1l3 during *Xenopus* eye development using the powerful antisense morpholino oligonucleotide (MO)-based knockdown approach. This approach does not induce genetic compensation as often observed when working with deleterious mutations (Blum et al., 2015; Rossi et al., 2015). To test the efficiency of Sipa1l3 MO, we cloned the Sipa1l3 MO-binding site (bs) in frame with and in front of *GFP* (Fig. S1A). Injection of the *sipa1l3 MO-bs GFP* together with the control MO resulted in GFP translation whereas the co-injection of the *sipa1l3 MO-bs GFP* with the Sipa1l3 MO efficiently blocked GFP translation in a MO dose dependent manner (Fig. S1B). Additionally, endogenous Sipa1l3 protein was reduced upon Sipa1l3 MO injection as shown by western blot (Fig. S1C).

To interfere with Sipa1l3 function during *Xenopus* eye development, we injected the Sipa1l3 MO unilaterally into the presumptive anterior neural tissue. As in all future experiments, 500 pg *GFP* RNA was co-injected to ensure injection was successful. Sipa1l3-deficient *Xenopus* embryos exhibited abnormalities during eye development, whereas wild-type embryos and embryos injected with control MO showed normally developed eyes (Fig. 2A,B). Sipa1l3 morphant embryos displayed significantly smaller eyes (Fig. 2A, white arrowheads; C,D) and lenses (Fig. 2E,F) as well as deformed eye structures including a reduced RPE (Fig. 2A, red arrowheads).

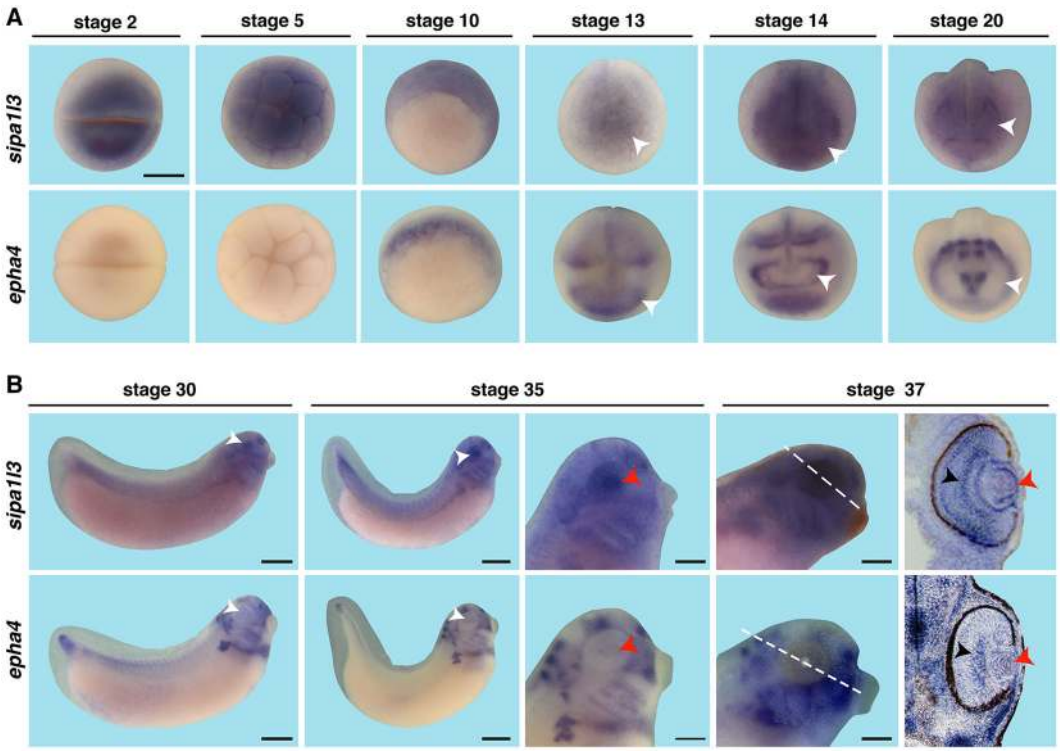

Fig. 1. Comparative gene expression of *sipa1l3* and *epha4*. (A) WMISH shows that *sipa1l3* and *epha4* are similarly expressed in the early eye field (white arrowheads). Scale bar: 500 µm. (B) *sipa1l3* and *epha4* are expressed in the developing eye (white arrowheads) including the retina (black arrowheads) and lens (red arrowheads). Dashed lines in B, stage 37 indicate level of transversal sections. Scale bars: 500 µm in stages 30/35; 250 µm in stages 35/37.

Development (2017) 144, 321-333 doi:10.1242/dev.147462

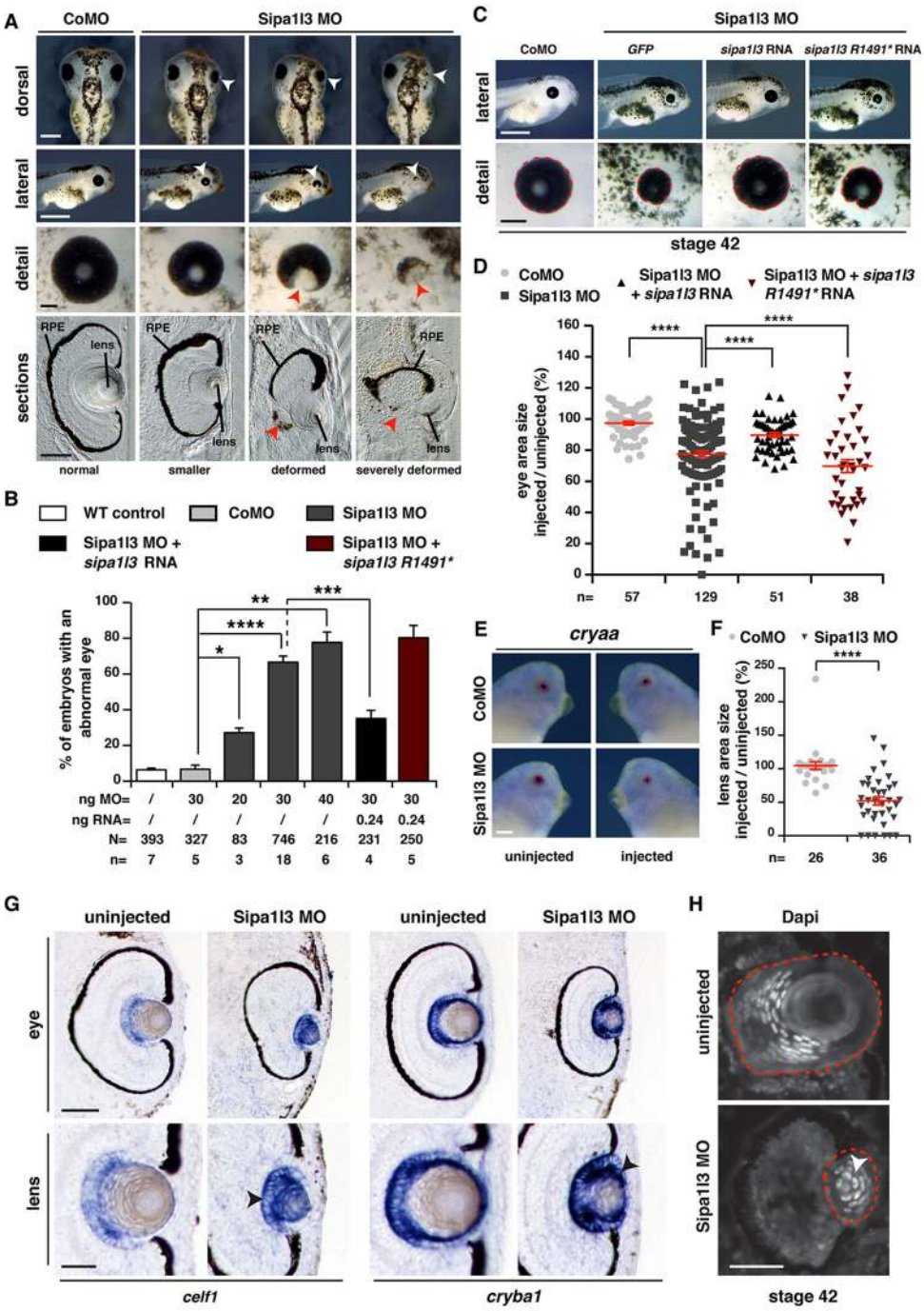

Fig. 2. Sipa1l3 is required for *Xenopus* ocular development. (A) Loss of Sipa1l3 through injection with Sipa1l3 MO leads to smaller and deformed eyes (white arrowheads) at stage 42, including a disturbed RPE (red arrowheads) in comparison with uninjected side and control MO (CoMO) injected embryos. Scale bars: 500 µm in dorsal views; 1000 µm in ventral views; 100 µm in detail and section views. (B) Quantification of data in A reveals an abnormal eye phenotype in a dose-dependent manner upon Sipa1l3 deficiency (dark gray columns). The Sipa1l3 MO phenotype was rescued by co-injecting a full-length rat *sipa1l3* RNA (black column) but not a mutated rat *sipa1l3 R1491** RNA (red column). The *sipa1l3 R1491** construct reflects the nonsense point mutations identified in human patients (Evers et al., 2015). (C) Measurement of the eye area size at stage 42. Red circles indicate the eye areas. Scale bars: 1000 µm in upper row; 200 µm in lower row. (D) Quantification of the data in C revealed a significant reduction in eye size upon Sipa1l3 depletion compared with control. Wild-type rat *sipa1l3* but not *sipa1l3 R1491** RNA restores the microphthalmia phenotype. (E) Lens area measurement of *cryaa*-stained embryos at stage 36 upon loss of Sipa1l3 compared with uninjected side and control MO-injected embryos. Note that the *cryaa* staining is not absent. Red circles indicate the lens area. Scale bar: 250 µm. (F) Quantification of the data in E revealed a significant reduction in lens size upon Sipa1l3 depletion. (G) Sipa1l3 MO injection does not reduce the expression of *celf1* and *cryba1* (black arrowheads). Scale bars: 100 µm in upper row; 50 µm in lower row. (H) DAPI staining on cryosections revealed nuclei in the lens center upon loss of Sipa1l3 (injected side, white arrowhead) whereas the uninjected side shows no nuclei in the lens center. The dotted line indicates the lenses. Scale bar: 50 µm. RPE, retinal pigmented epithelium; *N*, number of analyzed embryos in total; *n*, number of independent experiments; ng, nanogram. Error bars indicate standard error of the means (s.e.m.); **P*≤0.05; ***P*≤0.01; ****P*≤0.001; *****P*≤0.0001. *P*-values were calculated by a nonparametric, one-tailed Mann–Whitney rank sum test.

As *sipa1l3* is specifically expressed in the retina (Fig. 1A) and vibratome sections of Sipa1l3-depleted embryos indicated a disturbed retinal lamination (Fig. 2A, red arrowheads), we analyzed the lamination in more detail by staining for retinal cell type-specific markers (Cizelsky et al., 2013). All retinal cell types (photoreceptor, bipolar, ganglion and amacrine cells) were generated but the retinal layers were disorganized as photoreceptor cells were displaced in the inner retinal layers, forming rosette-like structures (Fig. S2A, red arrowheads). qPCR experiments (Fig. S2B) confirmed the induction of all cell types but indicated a mild shift in cellular fate from photoreceptor cells to the other analyzed retinal cell types.

We also examined the maturation of the lens fiber cells (LFCs) on a molecular and cellular level. For an examination on the molecular level, we stained Sipa1l3-depleted embryos for *celf1*, a specific marker for mature LFCs, and *cryba1*, a specific marker for the epithelial stem cell layer (Day and Beck, 2011) and prepared tissue sections. This analysis confirmed the reduction in lens size upon Sipa1l3 loss-of-function (LOF) and furthermore showed that neither *celf1* nor *cryba1* were downregulated (Fig. 2G, black arrowheads). qPCR data strengthened these observations. Whereas *cryba1* was not affected upon Sipa1l3 depletion, *celf1* was found to be upregulated in qPCR approaches (Fig. S3). The upregulation of *celf1* might be explained by a compensatory mechanism in response to the lens size reduction.

For an analysis on a cellular level, we performed DAPI staining on cryosections, which revealed an accumulation of light-scattering

Development (2017) 144, 321-333 doi:10.1242/dev.147462

nuclei in all regions of Sipa1l3-deficient lenses (Fig. 2H). These data indicate that the maturation of the lens is disturbed upon Sipa1l3 depletion, mainly due to cellular defects.

Furthermore, the Sipa1l3 MO-induced microphthalmia phenotype could be rescued by co-injection of Sipa1l3 MO with a full-length rat *Sipa1l3* RNA (Fig. 2B-D), which validates the specificity of the Sipa1l3 MO-induced eye phenotypes. Importantly, injection of Sipa1l3 MO together with a mutated rat *Sipa1l3 R1491** RNA (nonsense point mutation found in human patients; Evers et al., 2015) did not lead to a rescue of the observed phenotype (Fig. 2B-D).

Sipa1l3 interacts with Epha4

Ephrin signaling is one of the major pathways that determine ocular development (Cheng et al., 2013; Cooper et al., 2008). Since an interaction of the Sipa1l1 PDZ domain with Epha4 has already been reported (Richter et al., 2007), we analyzed the interaction of Sipa1l3 and Epha4. To this end, we overexpressed various Sipa1l3 constructs that encoded different sets of protein interaction domains in Cos7 cells and incubated those with the P2 fraction of mouse brain homogenate. We found that Epha4 protein interacted with the full-length Sipa1l3 and confirmed the known interaction with the PDZ domain (Fig. 3A). To substantiate these data, we co-expressed a Myc-tagged Sipa1l3 PDZ domain and the C-terminal end of Epha4 as a GFP fusion protein, and immunoprecipitated this molecular complex with GFP beads. Subsequently, we confirmed the interaction of these domains by western blotting (Fig. 3B,C). Finally, we investigated the localization of both the PDZ domain of Sipa1l3 and the C-terminal end of Epha4 after co-transfection in Cos7 cells. The overexpressed proteins co-localized and formed

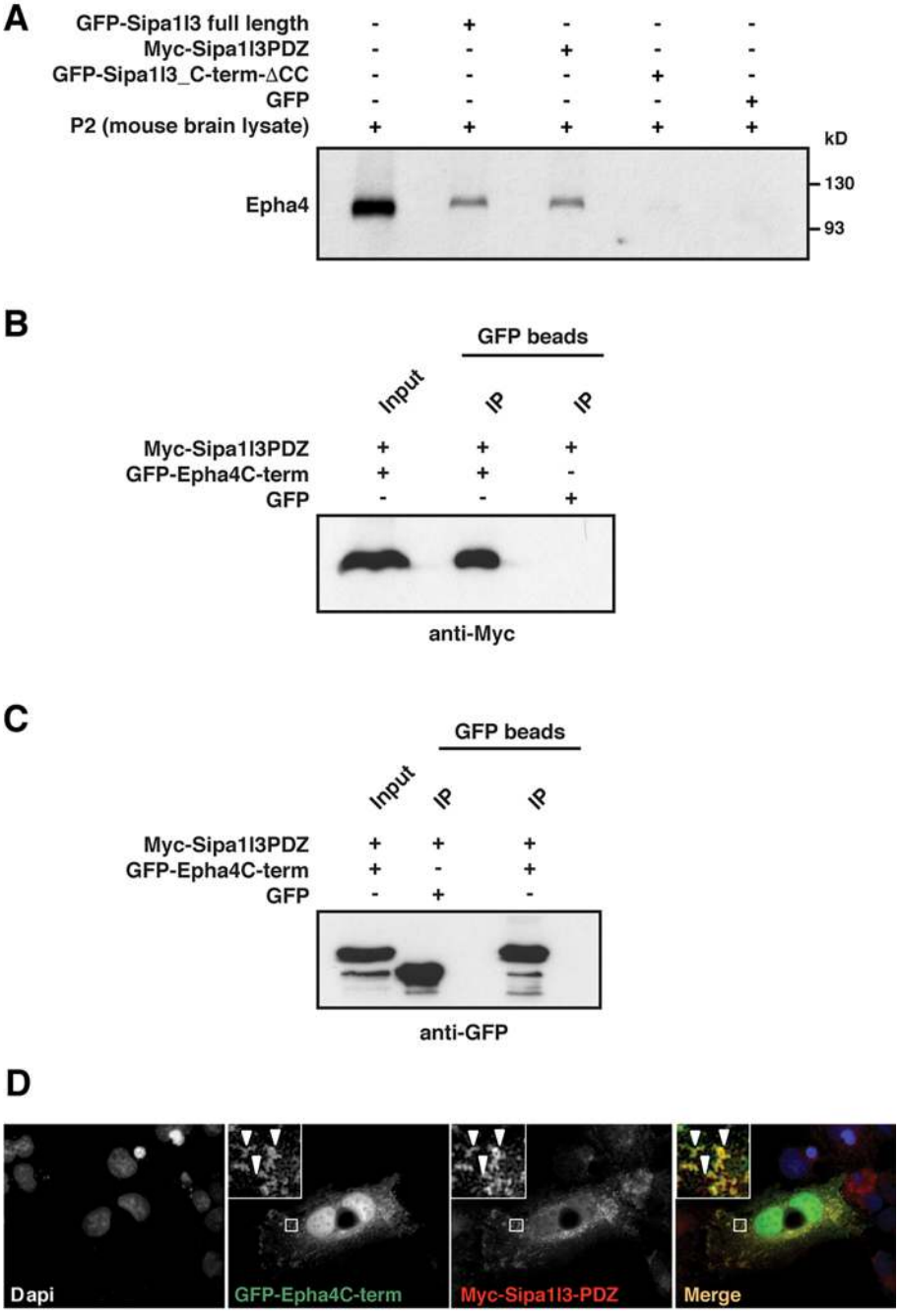

Fig. 3. Sipa1l3/Epha4 interaction. (A) Pulldown experiments using immunoprecipitated full-length GFP-Sipa1l3, Myc-Sipa1l3PDZ, GFP-Sipa1l3_C-term-CC, GFP and mouse brain lysate (P2 fraction) as indicated. Endogenous Epha4 was only pulled down by full-length GFP-Sipa1l3 and Myc-Sipa1l3PDZ. (B,C) Interaction of Sipa1l3 and Epha4 is shown by immunoprecipitation. (B) Anti-GFP beads were used for IP of the GFP-Epha4C-term/Myc-Sipa1l3PDZ interaction complex. Western blotting was performed with anti-Myc as indicated. (C) IP control was performed in an independent experiment with anti-GFP as indicated. (D) The interaction of Sipa1l3 and Epha4 was substantiated by co-transfection of both constructs in Cos7 cells followed by immunostaining with anti-Myc antibody. The GFP signal and the fluorescent staining of the Myc-tag show a complete overlay in cell clusters (white arrowheads).

Development (2017) 144, 321-333 doi:10.1242/dev.147462

large clusters within the cell soma (Fig. 3D). Furthermore, immunostaining of the Myc epitope revealed a clear co-localization of the Myc and GFP signals (Fig. 3D).

Loss of Epha4 receptor phenocopies loss of Sipa1l3 in *Xenopus*

Considering that Sipa1l3 interacts with the Epha4 receptor *in vitro*, we examined whether this interaction is of relevance *in vivo*. We started out by acquiring the expression profile of *epha4* in *Xenopus*. Whole-mount *in situ* hybridization (WMISH) analysis revealed a strong expression of *epha4* in the developing eye, including in the anterior neural field (Fig. 1A, lower row, white arrowheads), the retina (Fig. 1B, lower row, black arrowhead) and lens (Fig. 1B, lower row, red arrowhead). This expression pattern is similar to the expression profile of *sipa1l3* (compare with upper rows). By double WMISH, we further confirmed that *epha4* expression is localized at the border of the early eye field positive for *rax*, a transcription factor important for early eye development (Bailey et al., 2004) (Fig. S4).

Additionally, knockdown experiments of Epha4 using a functional Epha4 MO (Fig. S1D,E) resulted in similar eye defects as observed upon loss of Sipa1l3. Epha4 morphant embryos showed abnormal eyes (Fig. 4A,B) including a microphthalmia phenotype (Fig. 4A, white arrowheads; C,D), often accompanied by deformed eye structures (Fig. 4A, red arrowheads). In contrast, the uninjected control side, wild-types and control MO-injected embryos exhibited normal eye structures. Comparable with Sipa1l3-deficient embryos, loss of Epha4 resulted in disturbed retinal lamination and a mild fate shift of retinal cells as shown by WMISH and qPCR experiments (Fig. S2). Rescue experiments by co-injection of the Epha4 MO together with chicken *epha4* RNA that is not inhibited by the Epha4 MO (Fig. S1D,E) validated the specificity of the Epha4 MO-induced eye phenotype (Fig. 4B-D).

Furthermore, depletion of Epha4 led to a significant reduction in lens size (Fig. 4E,F). Sections of *Xenopus* embryos and qPCR showed expression of *celf1* and *cryba1* upon Epha4 depletion was similar to Sipa1l3 LOF (Fig. 4G, black arrowheads; Fig. S3). Additionally, we noticed an accumulation of nuclei in Epha4-deficient lenses, similar to what we observed after Sipa1l3 depletion (Fig. 4H).

Epha4 is upstream of Sipa1l3 during *Xenopus* eye development

To investigate whether the interaction between Sipa1l3 and Epha4 is of functional relevance *in vivo*, we injected a low dose of both MOs either alone or in combination. Intriguingly, low dose injections of Sipa1l3 or Epha4 MO led to a mild eye phenotype in a few embryos. Injection of both MOs in combination, however, led to a severe eye phenotype in a more than additive manner (Fig. 5A,B). This finding indicates a synergistic activity of both proteins and suggests that both proteins functionally act in the same signaling pathway.

As Epha4 is located at the cell membrane and Sipa1l3 is located in the cytoplasm close to the cell membrane (Dolnik et al., 2016), we hypothesized Epha4 to be functionally upstream of Sipa1l3. We performed rescue experiments by injecting the Epha4 MO together with rat *sipa1l3* RNA and observed a significant reduction in the number of embryos exhibiting eye abnormalities including the microphthalmia phenotype (Fig. 5C-E). The observed restoration of the eye by *sipa1l3* RNA in Epha4 morphants strengthens the conjecture that Epha4 acts upstream of Sipa1l3.

Loss of Sipa1l3 and Epha4 function influence early eye development

To examine the molecular basis of the microphthalmia phenotype upon Sipa1l3 or Epha4 knockdown, we analyzed how their depletion affects eye field induction (stage 13) and differentiation of eye-specific cells (stage 23). The unilateral injection of Sipa1l3 or Epha4 MO led to a strong reduction of the eye-specific markers *rax* and *pax6* at stage 13 and 23 (Fig. 6A-H). In contrast, control MO injections had no effect on eye markers. The pan-neural marker gene *sox3*, however, was not affected at stage 13 upon Sipa1l3 or Epha4 depletion, indicating a specific role for Sipa1l3 or Epha4 in the regulation of eye specification.

To investigate whether the ocular phenotype upon Sipa1l3 or Epha4 LOF is mediated through the downregulation of *rax*, we performed rescue experiments using *rax* RNA (Giannaccini et al., 2013). These experiments indeed showed that *rax* overexpression partially but significantly rescued the eye phenotype induced by knocking down Sipa1l3 or Epha4 (Fig. 6I-N). These results indicate that the microphthalmia ocular phenotype upon Epha4 and/or Sipa1l3 LOF is mediated at least in part through the downregulation of *rax*. Note that the injection of higher *rax* RNA doses induces ectopic RPE patches (Mathers et al., 1997).

One potential cause for the microphthalmia phenotype could be increased cell apoptosis. Thus, we performed TUNEL stainings in Sipa1l3-depleted whole embryos at stage 23 when marker genes are already reduced. These data revealed a significant increase in TUNEL-positive cells compared with control MO-injected embryos (Fig. S5), implicating cell apoptosis in the microphthalmia phenotype.

Interaction of Epha4 and Sipa1l3 causes proper eye development through β-catenin-independent Wnt signaling

In studies previously published by others, it has been shown that overexpression of β-catenin in LFCs results in an inhibition of LFC differentiation and cataract formation (Antosova et al., 2013; Shaham et al., 2009) that is similar to the Sipa1l3 LOF phenotype in the mouse (Greenlees et al., 2015). Gain of β-catenin function in the lens also leads to microphthalmia (Martinez et al., 2009) comparable to the loss of Sipa1l3 phenotype (Fig. 2C,D; Greenlees et al., 2015). Additionally, Sipa1l1 has been linked to Wnt/β-catenin signaling (Tsai et al., 2007). Therefore, we hypothesized that Sipa1l3 depletion leads to an upregulation of β-catenin during ocular development. Since it is well known that stabilization of β-catenin is involved in the upregulation of target gene expression by activating the TCF/LEF transcription factor complex in the nucleus (Rao and Kuhl, 2010), we assumed that downregulation of LEF activity should rescue the Sipa1l3 LOF eye phenotype. We therefore co-injected the Sipa1l3 MO together with a hormone-inducible dominant-negative (dn) LEF construct in *Xenopus* embryos. Expression of dnLEF was induced at stage 15 using dexamethasone. Intriguingly, inhibition of LEF significantly restored the Sipa1l3 MO-induced eye phenotype at stage 42 and eye marker gene expression at stage 23 (Fig. 7A-E). These results were supported by the finding that downregulation of either Sipa1l3 or Epha4 led to an upregulation of *axin2* expression, a well-known direct target gene of Wnt/β-catenin signaling (Jho et al., 2002), in neuralized animal cap cells at stage 13 (Fig. 7F).

Moreover, in a bimolecular-fluorescence (split YFP) complementation assay, we observed an interaction between the PDZ domain of Sipa1l3 and Dishevelled (Dsh, also known as Dvl), further supporting our hypothesis that Sipa1l3 is involved in Wnt

Development (2017) 144, 321-333 doi:10.1242/dev.147462

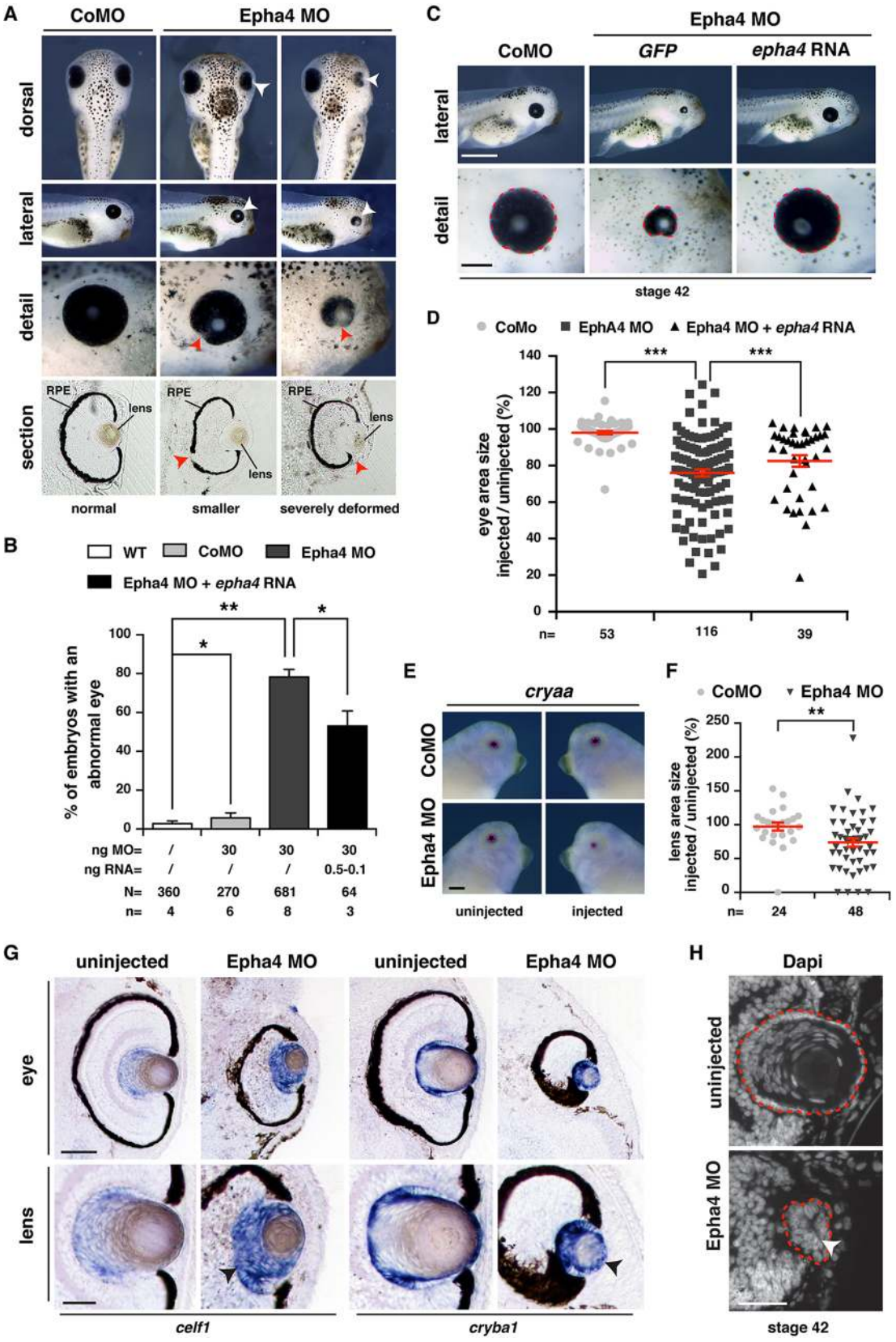

Fig. 4. See next page for legend.

signaling (Fig. 7G). It was recently demonstrated that the EphrinB1 receptor is involved in β-catenin-independent Wnt signaling during eye development (Lee et al., 2006). To test whether Epha4 and Sipa1l3 are also integrated into non-canoncial Wnt signaling, we made use of a well-described dsh deletion construct, *dshΔdix*, that promotes β-catenin-independent Wnt signaling branches. Indeed,

Development (2017) 144, 321-333 doi:10.1242/dev.147462

Fig. 4. Loss of Epha4 phenocopies the loss of Sipa1l3 in *Xenopus*. (A) Loss of Epha4 through injection with Epha4 MO phenocopies the eye phenotype upon Sipa1l3 deficiency including smaller and deformed eyes (white arrowheads) with disturbed RPE (red arrowheads) in comparison with uninjected side and control MO (CoMO). (B) Quantification of the data shown in A. The abnormal eye phenotype is rescued by *epha4* RNA co-injection (black column). (C) Measurement of eye area size at stage 42. Red circles indicate eye areas. Scale bars: 1000 µm in upper row; 200 µm in lower row. (D) Quantification of the data in C revealed a significant reduction in eye size upon Epha4 depletion. *Epha4* RNA restores the microphthalmia phenotype upon Epha4 depletion. (E) Lens area measurement of *cryaa*-stained embryos at stage 36 upon loss of Epha4 compared with uninjected side and control MO-injected embryos. Red circles indicate lens areas. Scale bar: 250 µm. Note that *cryaa* staining is not absent. (F) Quantification of the data in E revealed a significant reduction in lens size upon Epha4 depletion. (G) Epha4 MO injection does not reduce *celf1* and *cryba1* expression (black arrowheads). Scale bars: 100 µm in upper row; 50 µm in lower row. (H) DAPI staining on cryosections revealed nuclei in the lens after loss of Epha4 (injected side, white arrowhead), compared with internal control (uninjected side). The dotted lines indicate the lenses. Scale bar: 50 µm. *N*, number of analyzed embryos in total; *n*, number of independent experiments; ng, nanogram. Error bars indicate standard error of the means (s.e.m.); **P*≤0.05; ***P*≤0.01; ****P*≤0.001. *P*-values were calculated by a nonparametric, one-tailed Mann–Whitney rank sum test.

we found that the eye phenotype upon Sipa1l3 or Epha4 LOF could be significantly rescued by co-injecting *dshΔdix* RNA (Fig. 7H-M).

Taken together, we conclude that under normal physiological conditions the interaction between Sipa1l3 and Epha4 leads to the inhibition of Wnt/β-catenin signaling, accompanied by the activation of non-canonical Wnt signaling (Fig. 7N). In contrast, Sipa1l3 knockdown results in the stabilization of β-catenin that causes eye defects due to LEF activation and transcription of *axin2* (Fig. 7O).

DISCUSSION

Using *Xenopus* as model system, we further elucidated the molecular mechanisms that explain, at least in part, the cataract and microphthalmia phenotypes observed upon loss or mutation of the *Sipa1l3* gene in mice and humans. By rescue experiments, we showed the causative pathogenic relevance of Sipa1l3 LOF mutations observed in human patients and demonstrated that the interaction between Sipa1l3 and Epha4 is required for balancing canonical and non-canonical Wnt signaling during ocular development.

Sipa1l3 is required for ocular development

Besides its expression in neurons of the brain, Sipa1l3 is highly expressed in the mouse (Lachke et al., 2012), frog (this study and Rothe et al., 2016) and zebrafish (Greenlees et al., 2015) eye including in the retina and lens. Expression of the classically neuronal Sipa1l3 in lens tissue is not surprising considering the

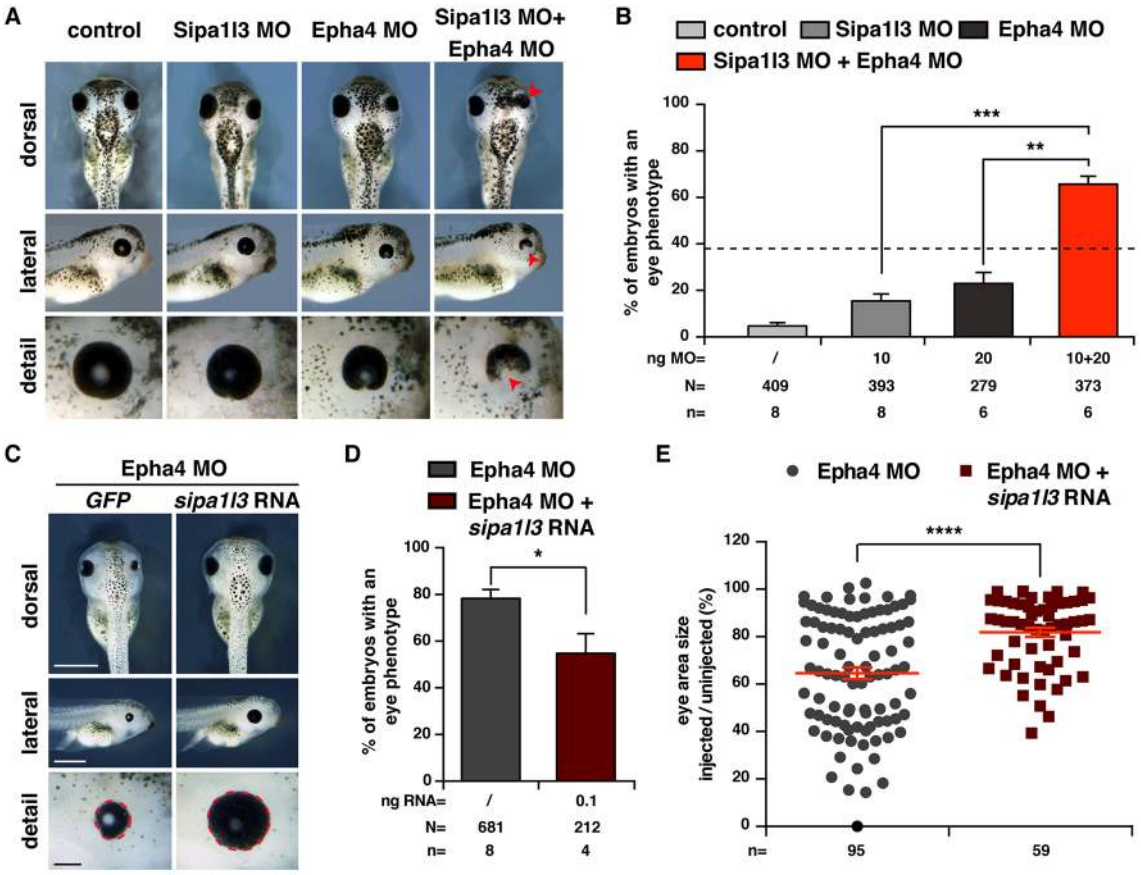

Fig. 5. Sipa1l3 acts downstream of Epha4 during *Xenopus* eye development. (A) Injection of Sipa1l3 and Epha4 MO showed a synergistic effect. Injection of low Sipa1l3 or Epha4 MO doses resulted in a mild eye phenotype in some embryos. Co-injection of both MOs, however, resulted in a severe eye phenotype in a more than additive manner. (B) Quantification of the data in A. (C) The eye phenotype upon Epha4 MO injection was rescued by *sipa1l3* RNA co-injection. Red circles indicate eye areas. (D) Quantification of the data in C. (E) Quantification of eye area size at stage 42 showed that *sipa1l3* RNA restores the microphthalmia phenotype resulting from Epha4 deficiency. *N*, number of analyzed embryos in total; *n*, number of independent experiments; ng, nanogram. Error bars indicate standard error of the means (s.e.m.); **P*≤0.05; ***P*≤0.01; ****P*≤0.001; *****P*≤0.0001. *P*-values were calculated by a nonparametric, one-tailed Mann–Whitney rank sum test.

Development (2017) 144, 321-333 doi:10.1242/dev.147462

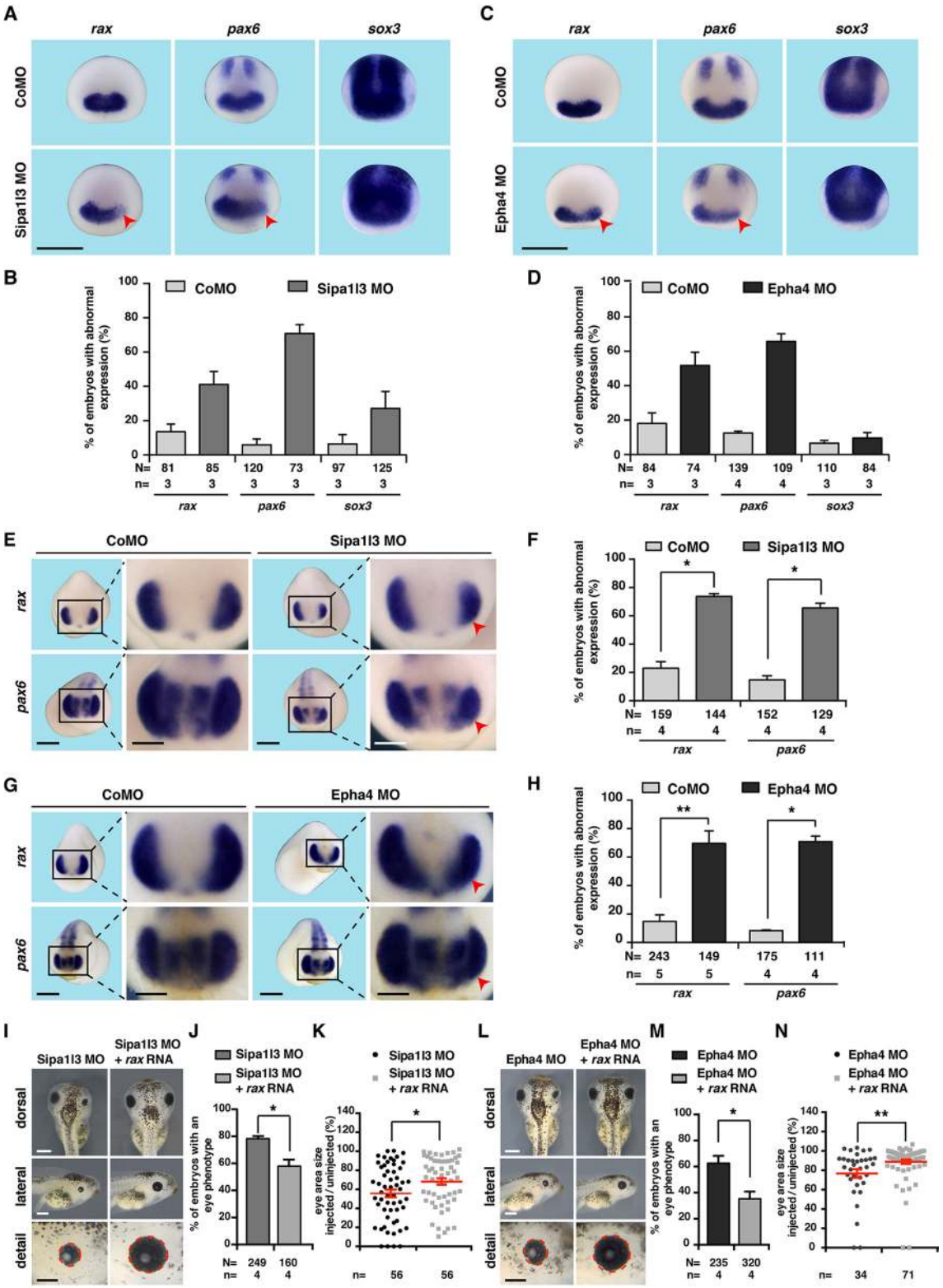

Fig. 6. Sipa1l3 and Epha4 influence early eye specification. (A,C) WMISH at stage 13 revealed that Sipa1l3 (A) or Epha4 (C) function is required for proper *rax* and *pax6* expression whereas *sox3* is not affected. Red arrowheads indicate reduced marker gene expression at the injected side. Scale bars: 1000 µm. (B,D) Quantification of the data in A,C. (E,G) Knockdown of Sipa1l3 (E) and Epha4 (G) resulted in significantly reduced *rax* and *pax6* expression domains (red arrowheads) compared with internal control as well as control MO-injected embryos at stage 23. Scale bars: 500 µm in overview; 250 µm in close-up views. (F,H) Quantification of the data in E,G. (I) *rax* RNA restores the Sipa1l3 MO-induced ocular phenotype. Red circles indicate eye areas. Scale bars: 500 µm in dorsal, lateral views; 250 µm in detail views. (J) Quantification of the data in I. (K) *rax* RNA rescues the Sipa1l3 MO-induced microphthalmia phenotype. (L) *rax* RNA restores the Epha4 MO-induced ocular phenotype. Red circles indicate eye areas. Scale bars: 500 µm in dorsal, lateral views; 250 µm in detail views. (M) Quantification of the data in L. (N) *rax* RNA rescues the Epha4 MO-induced microphthalmia phenotype. *N*, number of analyzed embryos in total; *n*, number of independent experiments. Error bars indicate standard error of the means (s.e.m.); $*P \leq 0.05$; $**P \leq 0.01$. *P*-values were calculated by a nonparametric, one-tailed Mann–Whitney rank sum test.

Development (2017) 144, 321-333 doi:10.1242/dev.147462

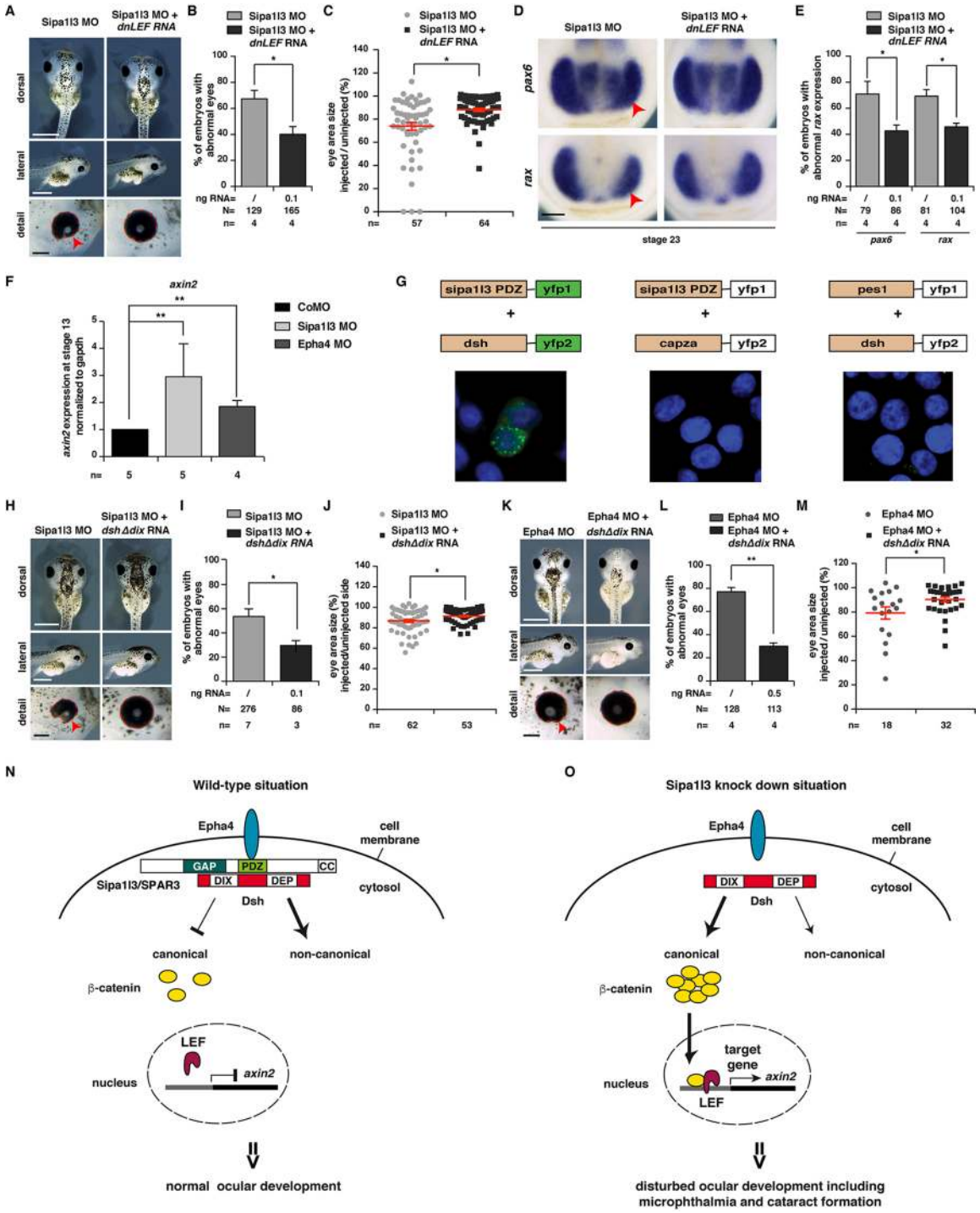

Fig. 7. Epha4 and Sipa1l3 act through non-canonical Wnt signaling. (A) Loss of Sipa1l3 function (red arrowhead) is rescued by co-injecting *dnLEF* RNA at stage 42. Red circles indicate eye areas. (B) Quantification of the data in A. (C) Injection of *dnLEF* RNA restores the microphthalmia phenotype induced by Sipa1l3 downregulation. (D) Marker gene reduction (red arrowhead) at stage 23 upon loss of Sipa1l3 is rescued by *dnLEF* RNA. Scale bar: 200 µm. (E) Quantification of the data in D. (F) *axin2* is upregulated upon Sipa1l3 or Epha4 depletion as shown by qPCR using cDNA of *Xenopus* neuralized ACs at stage 13. (G) Split YFP complementation assay. The PDZ domain of rat Sipa1l3 interacts with *Xenopus* Dsh. For negative controls, the interaction with unrelated proteins (CapZa and Pes1) was analyzed. (H) Loss of Sipa1l3 (red arrowhead) is rescued by *dshΔdix* RNA co-injection. Red circles indicate eye areas. Scale bar: 1000 µm in dorsal and lateral view; 200 µm in detail view. (I) Quantification of the data in H. (J) Injection of *dshΔdix* RNA restores the microphthalmia phenotype induced by Sipa1l3 downregulation. (K) Loss of Epha4 function (red arrowhead) is rescued by *dshΔdix* RNA co-injection. Red circles indicate lens areas. Scale bar: 1000 µm in dorsal and lateral view; 200 µm in detail view. (L) Quantification of the data in K. (M) Injection of *dshΔdix* RNA restores the microphthalmia phenotype induced by Epha4 depletion. (N) Scheme of the predicted mechanism in the wild-type situation. Interaction of Epha4 and Sipa1l3 leads to normal ocular development by blocking Wnt/β-catenin signaling and activation of the non-canonical Wnt pathway. (O) Scheme of the predicted mechanism in the Sipa1l3 loss-of-function situation. Sipa1l3 deficiency results in eye defects by upregulation of β-catenin and *axin2*. *N*, number of analyzed embryos in total; *n*, number of independent experiments; ng, nanogram. Error bars indicate standard error of the means (s.e.m.); **P*≤0.05; ***P*≤0.01. *P*-values were calculated by a nonparametric, one-tailed Mann–Whitney rank sum test.

Development (2017) 144, 321-333 doi:10.1242/dev.147462

common origin of the retina and the lens in the ectoderm of the early embryo. Studies have shown that many genes originally designated to be neuron-specific, such as synaptophysin or neuronal miRNA-124, are also expressed in the lens. Moreover, many cellular characteristics and mechanisms such as cellular structure and vesicle transport are quite comparable in neurons and LFCs (Frederikse et al., 2012).

To substantiate findings in the mouse that have been published by others and to analyze the underlying mechanism of the eye phenotype, we employed *Xenopus* as our model system. In a previous study, we confirmed the genomic conservation of the *sipa1l3* gene across species (Dolnik et al., 2016). Here, we showed a similar expression and function of Sipa1l3 in *Xenopus* compared with mouse and zebrafish (Greenlees et al., 2015; Lachke et al., 2012; Rothe et al., 2016). Consistent with the mouse model and human patients (Evers et al., 2015; Greenlees et al., 2015), eye and lens sizes were significantly reduced in Sipa1l3-deficient *Xenopus* embryos. Whereas the expression intensity of *cryaa* remained relatively normal in Sipa1l3-deficient embryos, the LFCs in the lens center still contained light-scattering nuclei, which provides an explanation for the cataract phenotype observed in human patients and the mouse model (Evers et al., 2015; Greenlees et al., 2015). We showed that loss of Sipa1l3 results in disturbed lens maturation. These findings are consistent with the observations by Greenlees et al. (2015) who showed an abnormal cell organization upon Sipa1l3 knock down.

By rescue experiments, we demonstrated that the rat *sipa1l3 R1491** RNA, which reflects the nonsense point mutation found in human patients with microphthalmia and congenital cataracts (Evers et al., 2015), does not restore the Sipa1l3 LOF eye phenotypes. This observation confirms the hypothesis put forward by Evers et al., (2015) who proposed that Sipa1l3 mutations are the underlying cause of the eye phenotype in human patients. As the missense point mutation (D148Y) had already been shown to be effective in cell culture experiments (Greenlees et al., 2015), we deemed it unnecessary to perform rescue experiments with that construct.

Possibilities for the microphthalmia phenotype upon Sipa1l3 suppression in human, mouse, frog and zebrafish could be a disturbed induction of the early neural plate and/or eye field, defects during eye-specific cell differentiation or increased cell apoptosis. To investigate these aspects, we used *Xenopus* embryos and analyzed marker gene expression at different stages. We observed defects as early as eye field induction as the eye-specific marker genes *pax6* and *rax* were strongly reduced upon loss of Sipa1l3. The pan-neural marker gene *sox3* was not reduced, showing the specific interference with eye-specific markers. As described by others, loss of *pax6* or *rax* leads to severe defects during eye development including microphthalmia (Bailey et al., 2004; Zuber et al., 2003). Moreover, we could show that *rax* overexpression results in a restoration of the ocular phenotype upon Sipa1l3 or Epha4 depletion, indicating that Sipa1l3 and Epha4 act via Rax during eye development. In addition, we are the first to report an increase in apoptosis upon Sipa1l3 depletion, which implicates apoptosis as one of the underlying causes for microphthalmia.

Sipa1l3 and Ephrin signaling

Given that Sipa1l1 interacts with Epha4 (Richter et al., 2007) and mutations in EphA2 as well as EfnA5 lead to cataracts (Cooper et al., 2008; Son et al., 2013), we investigated a possible interaction between Sipa1l3 and Epha4. Indeed, we showed that Sipa1l3 and Epha4 physically interact and propose a functional interplay of both proteins during ocular development. Accordingly, the expression pattern of *sipa1l3* and *epha4* in the *Xenopus* developing eye overlap to a considerable degree. Additionally, Epha4 downregulation resulted in an eye phenotype identical to that observed upon Sipa1l3 depletion. Synergy and rescue experiments showed that both molecules are indeed part of one signaling pathway during ocular development, with Epha4 acting upstream of Sipa1l3.

Despite the fact that both receptors (Epha2 and Epha4) are highly expressed in mouse lenses, cataract formation has only been described in *Epha2* knockout mice so far. It might well be that the lens phenotype in *Epha4* knockout mice that suffer from severe axonal pathfinding defects (Willi et al., 2012) is only mild and therefore might be overlooked. The retina and optic nerve phenotype has already been studied upon Epha4 downregulation (Helmbacher et al., 2000; Petros et al., 2006). It is, however, also conceivable that Epha2 compensates the loss of Epha4 in the murine *Epha4* knockout lens.

Sipa1l3 and Wnt signaling

We showed that inhibiting LEF rescued the eye phenotype upon loss of Sipa1l3. Additionally, Sipa1l3 or Epha4 deficiency resulted in an upregulation of the direct Wnt/β-catenin target *axin2*, which is in agreement with a previously published study that shows *axin2* overexpression upon Wnt/β-catenin activation in mouse lenses (Antosova et al., 2013). These observations fit very well to published data showing that cataract formation, smaller lenses and inhibited lens cell differentiation can be induced by β-catenin overexpression (Antosova et al., 2013; Shaham et al., 2009; Martinez et al., 2009). Note that overexpression of β-catenin in LFCs alone is sufficient to induce cataract formation (Antosova et al., 2013). Gain of β-catenin function in the central ocular ectoderm suppresses lens formation (Smith et al., 2005), which is in line with the smaller lenses found in our morphants. Thus, we propose that during normal ocular development, Epha4 and Sipa1l3 are required to inhibit Wnt/β-catenin signaling (Fig. 7N) (Fang et al., 2013). Moreover, we demonstrated that the Epha4 or Sipa1l3 MO eye phenotype can be rescued by activating non-canonical Wnt signaling. These findings suggest that Epha4 and Sipa1l3 positively regulate non-canonical Wnt signaling activity (Fig. 7N). This is in accordance with Greenlees et al. (2015) who showed that aPKC, a known mediator of non-canonical Wnt signaling, becomes ectopically localized in Sipa1l3-deficient Caco2 cells. Moreover, it is noteworthy to mention that non-canonical Wnt signaling antagonizes canonical Wnt signaling (Nemeth et al., 2007; Yuan et al., 2011). Whether Epha4 or Sipa1l3 inhibit β-catenin directly or indirectly via activating non-canonical Wnt activity has to be elucidated in the future.

MATERIALS AND METHODS

Xenopus laevis embryos

Xenopus embryos were obtained and cultured according to standard protocols (Sive et al., 2000) and staged as described (Nieuwkoop and Faber, 1956). *Xenopus* experiments were done in agreement with the German law and registered at the Regierungspräsidium Tuebingen.

Cloning

The open reading frame of rat Sipa1l3 (Dolnik et al., 2016) or chicken Epha4 was cloned into pCS2^{+} vector using *Sal*I or *Eco*RI (NEB). The point mutation at amino acid (aa) position 1491 (C>T; Sipa1l3_R1491*) was integrated, leading to a stop codon similar to that of human patients. To perform WMISH, the ORFs of an 893 bp (*sipa1l3*) and a 1.152 bp (*epha4*) fragment were cloned using cDNA isolated from *Xenopus* embryos of stages 25/37. Amplified DNA was ligated into the pSC-B vector (Agilent

Development (2017) 144, 321-333 doi:10.1242/dev.147462

Technologies). For the YFP assay, the PDZ domain of rat *Sipa1l3* (*Sipa1l3-PDZ*) and *Xenopus Dsh* (Yang-Snyder et al., 1996) were cloned in-frame into pVen1 or pVen2 vectors (Stöhr et al., 2006) using either *Eco*RI or SalI (New England Biolabs). *Sipa1l3* was fused to the N-terminal part of YFP (Ven1), whereas *Dsh* was fused to the N-terminal part of YFP (Ven2). For all amplifications, the proofreading Phusion DNA polymerase (Thermo Scientific, Waltham, MA, USA) was used. Clonings were confirmed by sequencing. For cloning primers see Table S1.

Biochemical and co-localization studies in Cos7 cells

Transfection and overexpression of different expression constructs GFP-Sipa1l3 full length, Myc-Sipa1l3PDZ, GFP-Sipa1l3_C-term-ΔCC and GFP-Epha4C-term was performed in Cos7 cells as previously described (Gessert et al., 2011) with minor modifications. PolyFect® (Qiagen) was used as transfection reagent according to the manufacturer's instructions. For biochemical experiments, extraction of proteins was performed using Triton X-100 lysis buffer (Miltenyi Biotech) at 4°C for 2 h with continuous shaking. Immunoprecipitation was performed using either anti-GFP or anti-Myc micro beads (Miltenyi Biotech) according to the manufacturers' instructions. For pulldown of endogenous Epha4, P2 fractions were obtained from adult mouse brain as previously described (Distler et al., 2014). Western blotting or immunohistochemistry was performed using standard protocols. Primary antibodies used were anti-Epha4 (1:1000; Invitrogen, 37-1600), anti-GFP (1:3000; BD Bioscience, 565197) and anti-Myc (1:3000; Roche, 11 667 149 001 and 11 667 203 001).

Morpholino oligonucleotides (MO) and RNA microinjections

MOs were purchased from Gene Tools, Philomath, OR, USA. MO sequences were Sipa1l3 MO: 5′-TCTGGTAAGATCTGAAACTTGTCA-T-3′; Epha4 MO: 5′-AGATGCCATGTACAATCCCAGCCAT-3′; control MO: 5′-CCTCTTACCTCAGTTACAATTTATA-3′. To test the efficiency of the Sipa1l3 MO, we injected 30-40 ng MO in total into 2-cell-stage embryos, cultured the embryos until stage 15, generated protein extracts and performed western blotting (Bugner et al., 2011) using anti-Sipa1l3 (1:1000; Abcam, ab113657) and anti-β tubulin isotype I and II (1:1000; Sigma, T8535) antibodies. To examine the binding efficiency of both MOs *in vivo*, the Sipa1l3 MO or Epha4 MO binding site (bs) were cloned in front of and in frame with GFP; see Table S1 for primers. Two-cell-stage embryos were injected with 1 ng *sipa1l3/epha4 MO-bs GFP* RNA, together with either 10 ng control MO or 0.1 ng, 0.5 ng or 1 ng Sipa1l3 and/or Epha4 MO, cultured until stage 26 and monitored under a fluorescence microscope (Olympus, M-VX, U-RFL-T, Japan). An Epha4 MO-bs mutant fusion construct was cloned and 1 ng *epha4 MO-bs mutant* RNA was co-injected with 10 ng Epha4 MO. To perform LOF experiments, we injected either 30 ng control MO, Sipa1l3 or Epha4 MO unilaterally into one animal-dorsal blastomere at the 8-cell stage to target anterior neural tissue. As lineage tracer, 0.5 ng *GFP* mRNA was co-injected (Schmeisser et al., 2013). Proper injection was confirmed at stages 13-20 using a fluorescence microscope. For rescue experiments, 30 or 50 ng Sipa1l3 or 30 ng Epha4 MO were co-injected with the corresponding RNA in following amounts: 0.1-0.24 ng rat *sipa1l3* RNA, 0.24 ng rat *sipa1l3_R1491** RNA, 0.1-0.5 ng chicken *epha4* RNA, 0.1 ng *Xenopus dnLEF* RNA, 0.1-0.5 ng *Xenopus dshΔdix* RNA (Miller et al., 1999) and 0.1-0.25 ng *Xenopus rax* RNA (Giannaccini et al., 2013). The hormone-inducible dnLEF construct (Deroo et al., 2004) was induced with 10 µM dexamethasone from stage 15 on. For synergy experiments, 10 ng Sipa1l3 and 20 ng Epha4 MO were unilaterally injected alone or in combination.

Eye and lens area measurement

MO injected and uninjected embryo sides were imaged using a SZX12 Olympus microscope at 16× magnification. ImageJ64/FIJI (NIH) was used for area calculations. Injected sides of individual embryos (LOF and rescue experiments) were calculated and compared with the uninjected side as well as with control MO injected embryos.

Whole-mount *in situ* hybridization (WMISH)

Digoxygenin-labeled antisense RNA probes were generated by *in vitro* transcription using T7 or T3 RNA polymerase (Roche). WMISH was performed according to established protocols (Hemmati-Brivanlou et al., 1990). Vibratome sections were performed as described (Gessert and Kühl, 2009).

Quantitative real-time polymerase chain reaction (qPCR)

For dissection of animal caps (ACs), two-cell-stage *Xenopus* embryos were bilaterally injected into the animal pole with either 50 ng control, Sipa1l3 MO or 30 ng Epha4 MO per cell. 600 pg noggin RNA per cell was co-injected to neuralize ACs. As lineage tracer, 500 pg GFP RNA was co-injected. At developmental stage 8.5-9, AC explants of 0.3×0.3 mm were dissected and cultured in 1× MBSH [10 mM HEPES, 88 mM NaCl, 1 mM KCl, 0.33 mM $Ca(NO_3)_2 \times (H_2O)_4$, 0.41 mM $CaCl_2 \times (H_2O)_4$, 0.82 mM $MgSO_4 \times (H_2O)7$, 2.4 mM $NaHCO_3$]/50 U/ml penicillin/0.05 mg/ml streptomycin at 12.5°C. A total of 10-16 ACs per approach were fixed at −80°C. To analyze gene expression in isolated *Xenopus* eyes, stage 42 embryo eyes injected with 15-20 Sipa1l3 MO, Epha4 MO or control MO, and matching uninjected eyes were isolated and fixed at −80°C. cDNA of ACs or isolated eyes diluted 1:10 was used to perform qPCR with a corresponding reverse transcriptase control. Gene expression levels were assessed using QuantiTect SYBR Green PCR Kit (Fermentas) on a Roche LightCycler 1.5 according to manufacturer's instructions. *gapdh* was used for normalization. For primer and PCR details see Table S2. qPCR calculations were performed using the ΔΔCP method (Livak and Schmittgen, 2001). In ACs, the ratio of the relative *axin2* expression was calculated for Sipa1l3 MO or Epha4 MO and compared with control MO. For stage 42 eyes, relative gene expression was calculated by comparing the injected to the uninjected side of each approach. In all qPCR experiments, *gapdh* was used for normalization.

TdT-mediated dUTP-biotin nick end labeling (TUNEL) staining

TUNEL staining was performed according to standard protocols (Gessert et al., 2007). TUNEL-positive cells were counted in defined areas at both sides of individual embryos.

Cryosectioning

Embryos were fixed in 1× PBS/4%PFA for 1 h at room temperature and equilibrated and cryo-sectioned as described (Fagotto, 1999). Sectioning was performed at a thickness of 10 µm using a Leica Frigocut 2800N cryostat microtome.

Split YFP complementation assay

To analyze the interaction between Sipa1l3-PDZ and Dsh *in vivo*, a split YFP (yellow fluorescent protein) complementation assay was performed in HEK293T cells (Tecza et al., 2011). For negative controls, the unrelated *Xenopus* Pes1 (Tecza et al., 2011) and murine CapZa were used.

Statistics

P-values were calculated by a nonparametric, one-tailed Mann–Whitney rank sum test using GraphPad Prism 6 software. Statistical significance is indicated as: $*P \leq 0.05$, $**P \leq 0.01$, $***P \leq 0.001$, $****P \leq 0.0001$.

Acknowledgements

We thank Astrid Pfister and Anna Dolnik for valuable discussions, Elena B. Pasquale (Sanford Burnham Prebys Medical Discovery Institute, CA, USA) and Massimiliano Andreazzoli (Institute of Biology at the University of Pisa, Italy) for providing plasmids. We thank Lisa Wischmann, Renate Zienecker and Jochen Kustermann for technical support. Special thanks to Helen Tauc for helpful comments on the manuscript.

Competing interests

The authors declare no competing or financial interests.

Author contributions

S.J.K. and M.K. designed all *Xenopus* experiments and the YFP complementation assay. M.R., P.D., S.J.K., N.K., F.A.S., A.H., A.L. and D.S. performed *Xenopus* experiments. A.H. and R.E. performed the YFP complementation assay. N.K., T.M.B., D.R. and J.B. designed and performed the Sipa1l3/Epha4 interaction experiments. S.J.K., M.K., T.M.B. and M.J.S. analyzed the data. S.J.K., M.K., M.R., T.M.B. and M.J.S. wrote the manuscript. All authors commented on the manuscript.

Funding
This study was supported by the International Graduate School in Molecular Medicine at the University of Ulm (GSC270).

Supplementary information
Supplementary information available online at
http://dev.biologists.org/lookup/doi/10.1242/dev.147462.supplemental

References

Antosova, B., Smolikova, J., Borkovcova, R., Strnad, H., Lachova, J., Machon, O. and Kozmik, Z. (2013). Ectopic activation of Wnt/beta-catenin signaling in lens fiber cells results in cataract formation and aberrant fiber cell differentiation. *PLoS ONE* **8**, e78279.
Bailey, T. J., El-Hodiri, H., Zhang, L., Shah, R., Mathers, P. H. and Jamrich, M. (2004). Regulation of vertebrate eye development by Rx genes. *Int. J. Dev. Biol.* **48**, 761-770.
Blum, M., De Robertis, E. M., Wallingford, J. B. and Niehrs, C. (2015). Morpholinos: antisense and sensibility. *Dev. Cell* **35**, 145-149.
Bugner, V., Tecza, A., Gessert, S. and Kuhl, M. (2011). Peter Pan functions independently of its role in ribosome biogenesis during early eye and craniofacial cartilage development in Xenopus laevis. *Development* **138**, 2369-2378.
Cheng, C., Ansari, M. M., Cooper, J. A. and Gong, X. (2013). EphA2 and Src regulate equatorial cell morphogenesis during lens development. *Development* **140**, 4237-4245.
Churchill, A. and Graw, J. (2011). Clinical and experimental advances in congenital and paediatric cataracts. *Philos. Trans. R. Soc. Lond. B Biol. Sci.* **366**, 1234-1249.
Cizelsky, W., Hempel, A., Metzig, M., Tao, S., Hollemann, T., Kühl, M. and Kühl, S. J. (2013). sox4 and sox11 function during Xenopus laevis eye development. *PLoS ONE* **8**, e69372.
Cooper, M. A., Son, A. I., Komlos, D., Sun, Y., Kleiman, N. J. and Zhou, R. (2008). Loss of ephrin-A5 function disrupts lens fiber cell packing and leads to cataract. *Proc. Natl. Acad. Sci. USA* **105**, 16620-16625.
Day, R. C. and Beck, C. W. (2011). Transdifferentiation from cornea to lens in Xenopus laevis depends on BMP signalling and involves upregulation of Wnt signalling. *BMC Dev. Biol.* **11**, 54.
Deroo, T., Denayer, T., Van Roy, F. and Vleminckx, K. (2004). Global inhibition of Lef1/Tcf-dependent Wnt signaling at its nuclear end point abrogates development in transgenic Xenopus embryos. *J. Biol. Chem.* **279**, 50670-50675.
Distler, U., Schmeisser, M. J., Pelosi, A., Reim, D., Kuharev, J., Weiczner, R., Baumgart, J., Boeckers, T. M., Nitsch, R., Vogt, J. et al. (2014). In-depth protein profiling of the postsynaptic density from mouse hippocampus using data-independent acquisition proteomics. *Proteomics* **14**, 2607-2613.
Dolnik, A., Kanwal, N., Mackert, S., Halbedl, S., Proepper, C., Bockmann, J., Schoen, M., Boeckers, T. M., Kühl, S. J. and Schmeisser, M. J. (2016). Sipa1l3/SPAR3 is targeted to postsynaptic specializations and interacts with the Fezzin ProSAPiP1/Lzts3. *J. Neurochem.* **136**, 28-35.
Evers, C., Paramasivam, N., Hinderhofer, K., Fischer, C., Granzow, M., Schmidt-Bacher, A., Eils, R., Steinbeisser, H., Schlesner, M. and Moog, U. (2015). SIPA1L3 identified by linkage analysis and whole-exome sequencing as a novel gene for autosomal recessive congenital cataract. *Eur. J. Hum. Genet.* **23**, 1627-1633.
Fagotto, F. (1999). The Wnt pathway in Xenopus development. In *Signaling through Cell Adhesion* (ed. J.-L. Guan), pp. 303-356. Boca Raton: CRC Press.
Fang, Y., Cho, K.-S., Tchedre, K., Lee, S. W., Guo, C., Kinouchi, H., Fried, S., Sun, X. and Chen, D. F. (2013). Ephrin-A3 suppresses Wnt signaling to control retinal stem cell potency. *Stem Cells* **31**, 349-359.
Frederikse, P. H., Kasinathan, C. and Kleiman, N. J. (2012). Parallels between neuron and lens fiber cell structure and molecular regulatory networks. *Dev. Biol.* **368**, 255-260.
Gessert, S. and Kühl, M. (2009). Comparative gene expression analysis and fate mapping studies suggest an early segregation of cardiogenic lineages in Xenopus laevis. *Dev. Biol.* **334**, 395-408.
Gessert, S., Maurus, D., Rössner, A. and Kühl, M. (2007). Pescadillo is required for Xenopus laevis eye development and neural crest migration. *Dev. Biol.* **310**, 99-112.
Gessert, S., Schmeisser, M. J., Tao, S., Boeckers, T. M. and Kühl, M. (2011). The spatio-temporal expression of ProSAP/shank family members and their interaction partner LAPSER1 during Xenopus laevis development. *Dev. Dyn.* **240**, 1528-1536.
Giannaccini, M., Giudetti, G., Biasci, D., Mariotti, S., Martini, D., Barsacchi, G. and Andreazzoli, M. (2013). Brief report: Rx1 defines retinal precursor identity by repressing alternative fates through the activation of TLE2 and Hes4. *Stem Cells* **31**, 2842-2847.
Greenlees, R., Mihelec, M., Yousoof, S., Speidel, D., Wu, S. K., Rinkwitz, S., Prokudin, I., Perveen, R., Cheng, A., Ma, A. et al. (2015). Mutations in SIPA1L3 cause eye defects through disruption of cell polarity and cytoskeleton organization. *Hum. Mol. Genet.* **24**, 5789-5804.
Gupta, V. B., Rajagopala, M. and Ravishankar, B. (2014). Etiopathogenesis of cataract: an appraisal. *Indian J. Ophthalmol.* **62**, 103-110.
Helmbacher, F., Schneider-Maunoury, S., Topilko, P., Tiret, L. and Charnay, P. (2000). Targeting of the EphA4 tyrosine kinase receptor affects dorsal/ventral pathfinding of limb motor axons. *Development* **127**, 3313-3324.
Hemmati-Brivanlou, A., Frank, D., Bolce, M. E., Brown, B. D., Sive, H. L. and Harland, R. M. (1990). Localization of specific mRNAs in Xenopus embryos by whole-mount in situ hybridization. *Development* **110**, 325-330.
Huot, J. (2004). Ephrin signaling in axon guidance. *Prog. Neuropsychopharmacol. Biol. Psychiatry* **28**, 813-818.
Jho, E.-H., Zhang, T., Domon, C., Joo, C.-K., Freund, J.-N. and Costantini, F. (2002). Wnt/beta-catenin/Tcf signaling induces the transcription of Axin2, a negative regulator of the signaling pathway. *Mol. Cell. Biol.* **22**, 1172-1183.
Jun, G., Guo, H., Klein, B. E. K., Klein, R., Wang, J. J., Mitchell, P., Miao, H., Lee, K. E., Joshi, T., Buck, M. et al. (2009). EPHA2 is associated with age-related cortical cataract in mice and humans. *PLoS Genet.* *5*, e1000584.
Lachke, S. A., Ho, J. W. K., Kryukov, G. V., O'Connell, D. J., Aboukhalil, A., Bulyk, M. L., Park, P. J. and Maas, R. L. (2012). iSyTE: integrated Systems Tool for Eye gene discovery. *Invest. Ophthalmol. Vis. Sci.* **53**, 1617-1627.
Lee, H.-S., Bong, Y.-S., Moore, K. B., Soria, K., Moody, S. A. and Daar, I. O. (2006). Dishevelled mediates ephrinB1 signalling in the eye field through the planar cell polarity pathway. *Nat. Cell Biol.* **8**, 55-63.
Livak, K. J. and Schmittgen, T. D. (2001). Analysis of relative gene expression data using real-time quantitative PCR and the 2(-Delta Delta C(T)) Method. *Methods* **25**, 402-408.
Lovicu, F. J. and McAvoy, J. W. (2005). Growth factor regulation of lens development. *Dev. Biol.* **280**, 1-14.
Lovicu, F. J., McAvoy, J. W. and de Iongh, R. U. (2011). Understanding the role of growth factors in embryonic development: insights from the lens. *Philos. Trans. R. Soc. Lond. B Biol. Sci.* **366**, 1204-1218.
Martinez, G. and de Iongh, R. U. (2010). The lens epithelium in ocular health and disease. *Int. J. Biochem. Cell Biol.* **42**, 1945-1963.
Martinez, G., Wijesinghe, M., Turner, K., Abud, H. E., Taketo, M. M., Noda, T., Robinson, M. L. and de Iongh, R. U. (2009). Conditional mutations of beta-catenin and APC reveal roles for canonical Wnt signaling in lens differentiation. *Invest. Ophthal. Vis. Sci.* **50**, 4794-4806.
Mathers, P. H., Grinberg, A., Mahon, K. A. and Jamrich, M. (1997). The Rx homeobox gene is essential for vertebrate eye development. *Nature* **387**, 603-607.
Miller, J. R., Rowning, B. A., Larabell, C. A., Yang-Snyder, J. A., Bates, R. L. and Moon, R. T. (1999). Establishment of the dorsal-ventral axis in Xenopus embryos coincides with the dorsal enrichment of dishevelled that is dependent on cortical rotation. *J. Cell Biol.* **146**, 427-437.
Nemeth, M. J., Topol, L., Anderson, S. M., Yang, Y. and Bodine, D. M. (2007). Wnt5a inhibits canonical Wnt signaling in hematopoietic stem cells and enhances repopulation. *Proc. Natl. Acad. Sci. USA* **104**, 15436-15441.
Nieuwkoop, P. D. and Faber, J. (1956). *Normal Table of Xenopus laevis (Daudin); A Systematical and Chronological Survey of the Development from the Fertilized Egg till the End of Metamorphosis*. Amsterdam: North-Holland Pub. Co.
Pak, D. T. S., Yang, S., Rudolph-Correia, S., Kim, E. and Sheng, M. (2001). Regulation of dendritic spine morphology by SPAR, a PSD-95-associated RapGAP. *Neuron* **31**, 289-303.
Pasquale, E. B. (2005). Eph receptor signalling casts a wide net on cell behaviour. *Nat. Rev. Mol. Cell Biol.* **6**, 462-475.
Petros, T. J., Williams, S. E. and Mason, C. A. (2006). Temporal regulation of EphA4 in astroglia during murine retinal and optic nerve development. *Mol. Cell. Neurosci.* **32**, 49-66.
Rao, T. P. and Kuhl, M. (2010). An updated overview on Wnt signaling pathways: a prelude for more. *Circ. Res.* **106**, 1798-1806.
Richter, M., Murai, K. K., Bourgin, C., Pak, D. T. and Pasquale, E. B. (2007). The EphA4 receptor regulates neuronal morphology through SPAR-mediated inactivation of Rap GTPases. *J. Neurosci.* **27**, 14205-14215.
Rossi, A., Kontarakis, Z., Gerri, C., Nolte, H., Hölper, S., Krüger, M. and Stainier, D. Y. R. (2015). Genetic compensation induced by deleterious mutations but not gene knockdowns. *Nature* **524**, 230-233.
Rothe, M., Monteiro, F., Dietmann, P. and Kühl, S. J. (2016). Comparative expression study of sipa family members during early Xenopus laevis development. *Dev. Genes Evol.* **226**, 369-382.
Schmeisser, M. J., Kühl, S. J., Schoen, M., Beth, N. H., Weis, T. M., Grabrucker, A. M., Kühl, M. and Boeckers, T. M. (2013). The Nedd4-binding protein 3 (N4BP3) is crucial for axonal and dendritic branching in developing neurons. *Neural Dev.* **8**, 18.
Shaham, O., Smith, A. N., Robinson, M. L., Taketo, M. M., Lang, R. A. and Ashery-Padan, R. (2009). Pax6 is essential for lens fiber cell differentiation. *Development* **136**, 2567-2578.
Shi, Y., De Maria, A., Bennett, T., Shiels, A. and Bassnett, S. (2012). A role for epha2 in cell migration and refractive organization of the ocular lens. *Invest. Ophthalmol. Vis. Sci.* **53**, 551-559.

Development (2017) 144, 321-333 doi:10.1242/dev.147462

Sive, H. L., Grainger, R. M. and Harland, R. M. (2000). *Early Development of Xenopus laevis: A Laboratory Manual*. Cold Spring Harbor, NY: Cold Spring Harbor Laboratory Press.

Smith, A. N., Miller, L.-A. D., Song, N., Taketo, M. M. and Lang, R. A. (2005). The duality of beta-catenin function: a requirement in lens morphogenesis and signaling suppression of lens fate in periocular ectoderm. *Dev. Biol.* **285**, 477-489.

Son, A. I., Cooper, M. A., Sheleg, M., Sun, Y., Kleiman, N. J. and Zhou, R. (2013). Further analysis of the lens of ephrin-A5$^{-/-}$ mice: development of postnatal defects. *Mol. Vis.* **19**, 254-266.

Spilker, C. and Kreutz, M. R. (2010). RapGAPs in brain: multipurpose players in neuronal Rap signalling. *Eur. J. Neurosci.* **32**, 1-9.

Spilker, C., Acuna Sanhueza, G. A., Bockers, T. M., Kreutz, M. R. and Gundelfinger, E. D. (2008). SPAR2, a novel SPAR-related protein with GAP activity for Rap1 and Rap2. *J. Neurochem.* **104**, 187-201.

Stöhr, N., Lederer, M., Reinke, C., Meyer, S., Hatzfeld, M., Singer, R. H. and Hüttelmaier, S. (2006). ZBP1 regulates mRNA stability during cellular stress. *J. Cell Biol.* **175**, 527-534.

Tecza, A., Bugner, V., Kühl, M. and Kühl, S. J. (2011). Pescadillo homologue 1 and Peter Pan function during Xenopus laevis pronephros development. *Biol. Cell* **103**, 483-498.

Tsai, I.-C., Amack, J. D., Gao, Z.-H., Band, V., Yost, H. J. and Virshup, D. M. (2007). A Wnt-CKIvarepsilon-Rap1 pathway regulates gastrulation by modulating SIPA1L1, a Rap GTPase activating protein. *Dev. Cell* **12**, 335-347.

Wederell, E. D. and de Iongh, R. U. (2006). Extracellular matrix and integrin signaling in lens development and cataract. *Semin. Cell Dev. Biol.* **17**, 759-776.

Wendholt, D., Spilker, C., Schmitt, A., Dolnik, A., Smalla, K.-H., Proepper, C., Bockmann, J., Sobue, K., Gundelfinger, E. D., Kreutz, M. R. et al. (2006). ProSAP-interacting protein 1 (ProSAPiP1), a novel protein of the postsynaptic density that links the spine-associated Rap-Gap (SPAR) to the scaffolding protein ProSAP2/Shank3. *J. Biol. Chem.* **281**, 13805-13816.

Willi, R., Winter, C., Wieske, F., Kempf, A., Yee, B. K., Schwab, M. E. and Singer, P. (2012). Loss of EphA4 impairs short-term spatial recognition memory performance and locomotor habituation. *Genes Brain Behav.* **11**, 1020-1031.

Wride, M. A. (2011). Lens fibre cell differentiation and organelle loss: many paths lead to clarity. *Philos. Trans. R. Soc. Lond. B Biol. Sci.* **366**, 1219-1233.

Yang-Snyder, J., Miller, J. R., Brown, J. D., Lai, C.-J. and Moon, R. T. (1996). A frizzled homolog functions in a vertebrate Wnt signaling pathway. *Curr. Biol.* **6**, 1302-1306.

Yuan, Y., Niu, C. C., Deng, G., Li, Z. Q., Pan, J., Zhao, C., Yang, Z. L. and Si, W. K. (2011). The Wnt5a/Ror2 noncanonical signaling pathway inhibits canonical Wnt signaling in K562 cells. *Int. J. Mol. Med.* **27**, 63-69.

Zuber, M. E., Gestri, G., Viczian, A. S., Barsacchi, G. and Harris, W. A. (2003). Specification of the vertebrate eye by a network of eye field transcription factors. *Development* **130**, 5155-5167.